JCI insight

The TBK1/IKKε inhibitor amlexanox improves dyslipidemia and prevents atherosclerosis

Peng Zhao, … , Joseph L. Witztum, Alan R. Saltiel

JCI Insight. 2022. https://doi.org/10.1172/jci.insight.155552.

Research In-Press Preview **Metabolism**

Cardiovascular diseases, especially atherosclerosis and its complications, are a leading cause of death. Inhibition of the non-canonical IκB kinases TBK1 and IKKε with amlexanox restores insulin sensitivity and glucose homeostasis in diabetic mice and human subjects. Here we report that amlexanox improves diet-induced hypertriglyceridemia and hypercholesterolemia in Western diet (WD)-fed *Ldlr*$^{-/-}$ mice, and protects against atherogenesis. Amlexanox ameliorates dyslipidemia, inflammation and vascular dysfunction through synergistic actions that involve upregulation of bile acid synthesis to increase cholesterol excretion. Transcriptomic profiling demonstrates an elevated expression of key bile acid synthesis genes. Furthermore, we found that amlexanox attenuates monocytosis, eosinophilia and vascular dysfunction during WD-induced atherosclerosis. These findings demonstrate the potential of amlexanox as a new therapy for hypercholesterolemia and atherosclerosis.

The TBK1/IKKε Inhibitor Amlexanox Improves Dyslipidemia and Prevents Atherosclerosis

Authors: Peng Zhao[1,2,3,9 *], Xiaoli Sun[2,3,4,5,9], Zhongji Liao[3], Hong Yu[4], Dan Li[1], Zeyang Shen[6,7], Christopher K. Glass[3,6], Joseph L. Witztum[3], Alan R. Saltiel[3,8 *]

Affiliations:

1. Department of Biochemistry and Structural Biology, University of Texas Health Science Center at San Antonio, San Antonio, TX 78229
2. Mays Cancer Center, University of Texas Health Science Center at San Antonio, San Antonio, TX 78229
3. Department of Medicine, University of California San Diego, La Jolla, CA 92093
4. Department of Pharmacology, University of Texas Health Science Center at San Antonio, San Antonio, TX 78229
5. Transplant Center, University of Texas Health Science Center at San Antonio, San Antonio, TX 78229
6. Department of Cellular and Molecular Medicine, School of Medicine, University of California San Diego, La Jolla, CA 92093
7. Department of Bioengineering, Jacob School of Engineering, University of California San Diego, La Jolla, CA 92093
8. Department of Pharmacology, School of Medicine, University of California San Diego, La Jolla, CA 92093
9. These authors contributed equally: Peng Zhao, Xiaoli Sun

* Correspondence to asaltiel@health.ucsd.edu or zhaop@uthscsa.edu

Alan Saltiel: 9500 Gilman Drive, La Jolla, CA 92093. Phone: 858-534-5953

Peng Zhao: 7703 Floyd Curl Drive, San Antonio, TX 78229. Phone: 210-567-3772

Abstract

Cardiovascular diseases, especially atherosclerosis and its complications, are a leading cause of death. Inhibition of the non-canonical IκB kinases TBK1 and IKKε with amlexanox restores insulin sensitivity and glucose homeostasis in diabetic mice and human subjects. Here we report that amlexanox improves diet-induced hypertriglyceridemia and hypercholesterolemia in Western diet (WD)-fed *Ldlr*$^{-/-}$ mice, and protects against atherogenesis. Amlexanox ameliorates dyslipidemia, inflammation and vascular dysfunction through synergistic actions that involve upregulation of bile acid synthesis to increase cholesterol excretion. Transcriptomic profiling demonstrates an elevated expression of key bile acid synthesis genes. Furthermore, we found that amlexanox attenuates monocytosis, eosinophilia and vascular dysfunction during WD-induced atherosclerosis. These findings demonstrate the potential of amlexanox as a new therapy for hypercholesterolemia and atherosclerosis.

Introduction

Metabolic diseases have become a worldwide epidemic (1). Atherosclerosis and its complications, including heart attack and stroke, are the leading causes of death (2,3). The origins of atherosclerosis are complex and multifactorial, and often linked via common underlying mechanisms. For example, hypercholesterolemia and hypertriglyceridemia are frequently associated with chronic inflammation, leading to excessive accumulation of monocyte-derived macrophages in the arterial wall that contributes to the development of atherosclerotic plaques (2,4-6). Atherosclerosis is currently treated primarily with statins, ezetimibe and PCSK9 inhibitors to decrease plasma cholesterol (7-10). Niacin was also shown to decrease LDL-cholesterol and increase HDL-cholesterol (11-13). However, the use of these agents is not always optimally efficacious and at times associated with problems. Some individuals cannot tolerate statins, the most widely used agents, due to myopathies and occasionally increased blood glucose and

insulin resistance (14-16). Other drugs that reduce triglycerides (Fibrates) or decrease bile acid reabsorption (bile acids sequestrants) are not as effective as statins, and carry other liabilities (17-19). While novel convertase subtilisin kexin type 9 (PCSK9) inhibitors, alirocumab and evolocumab, have recently been introduced to control cholesterol in patients who do not respond to statins, these drugs are expensive (20-22). Thus, there is a need for new safe and effective drugs to combat this devastating disease.

Obesity is characterized by low grade, persistent inflammation in adipose tissue and liver, involving the recruitment and activation of pro-inflammatory immune cells (23-25). These inflammatory events are characterized by activation of the transcriptional factor NFκB in both immune cells and metabolically active hepatocytes and adipocytes, linking obesity to both cardiovascular and metabolic disease (26-29). Studies from our laboratory on the NFκB pathway in adipose tissue and liver from obese mice revealed that both the noncanonical IκB kinases (IKKs), IKKε and TANK-binding kinase 1 (TBK1) are elevated in obesity due to NFκB activation, and further that both proteins play a role in suppressing energy expenditure in the obese state (28,30). These findings led us to discover amlexanox as a specific inhibitor of both kinases (30). This drug was developed in the mid-1980's to treat asthma and allergic rhinitis (31,32), and has an excellent record of safety. We demonstrated that amlexanox substantially improved glucose tolerance, fatty liver and insulin sensitivity, and reduced hepatic steatosis in genetically obese and diet-induced obese (DIO) mice (30,33,34), and significantly reduced HbA1c levels in a subset of diabetic patients with high basal levels of systemic inflammation (35). Mechanistic studies revealed that amlexanox reduced expression of pro-inflammatory cytokines genes *Ccl2*, *Ccl3*, and attenuated inflammation (30). Moreover, amlexanox inhibits IKKε-induced activation of phosphodiesterase 3B (PDE3B) to elevate cAMP levels and p38 phosphorylation in adipocytes, and thus increases catecholamine sensitivity and energy expenditure via increased adipose tissue browning and thermogenesis (36,37). However, it is unknown whether amlexanox could affect other diet-induced metabolic diseases, especially atherosclerosis. In this study, we assessed the effects of amlexanox on

Western diet (WD)-induced atherosclerosis in *Ldlr*$^{-/-}$ mice. We examined its effects on lipid metabolism, inflammation and vascular dysfunction, and demonstrate that amlexanox systemically ameliorates three major pathogenic mechanisms that promote atherogenesis. Given its beneficial effects in obesity, diabetes and fatty liver diseases, here we demonstrate the potential of amlexanox as a simultaneous treatment for atherosclerosis and other metabolic diseases, including diabetes and fatty liver disease.

Results

Amlexanox improves dyslipidemia and protects against atherosclerosis.

Amlexanox is a selective inhibitor of the protein kinases TBK1 and IKKε (30), and its administration to obese rodents or humans improved energy and glucose metabolism (30,35). To examine whether amlexanox exerts a beneficial effect on Western diet (WD)-induced atherosclerosis, we fed *Ldlr*$^{-/-}$ mice with WD for 3 weeks, and then orally gavaged the mice with vehicle or amlexanox for 8 weeks with the continuation of WD feeding (Figure 1A). Consistent with our previous findings, amlexanox improved diet-induced obesity, indicated by significantly reduced body weight and adipose tissue weight in WD-fed mice (Supplementary Figure 1B-1D). After 11 weeks of WD feeding, aortas were collected to evaluate lesion development. *En face* staining demonstrated that amlexanox substantially reduced the area of aortic lesions (Figure 1B-1C). Staining of aortic roots also showed that amlexanox significantly reduced the size of lesions (Figure 1D-1E). Together, these data demonstrated that amlexanox reduced atherogenesis in WD-fed *Ldlr*$^{-/-}$ mice.

Our previous studies demonstrated that amlexanox reduced blood glucose and improved insulin sensitivity in *ob/ob* and high fat diet (HFD)-fed mice (30). We thus examined the impact of amlexanox on diet-induced dyslipidemia, including hypertriglyceridemia and hypercholesterolemia. We found that mice gavaged with amlexanox had clear serum, while serum from mice in the vehicle group was milky (Figure 1F), indicating a robust reduction in serum lipid content in response to the drug. Measurement of

circulating levels of triglycerides and cholesterol demonstrated that 8 week gavage of amlexanox significantly reduced both triglycerides and cholesterol in WD-fed *Ldlr*$^{-/-}$ mice (Figure 1G-1H). Fast performance liquid chromatography (FPLC) analysis indicated that amlexanox reduced both VLDL-cholesterol and LDL-cholesterol, and slightly increased HDL-cholesterol. VLDL-triglycerides were also significantly reduced by amlexanox (Figure 1I-1J). Moreover, amlexanox significantly reduced liver weight (Supplementary Figure 1E), and H&E staining indicated an improvement of hepatic steatosis (Supplementary Figure 1F). Measurement of hepatic lipid content further confirmed a dramatic reduction of both triglycerides and cholesterol by amlexanox in WD-fed *Ldlr*$^{-/-}$ mice (Figure 1K-1L). In normal chow diet-fed *Ldlr*$^{-/-}$ mice, amlexanox showed no effects of serum cholesterol and triglyceride (Supplementary Figure 1G-1H). These data demonstrated that amlexanox significantly reduced triglycerides and cholesterol in both blood and liver of WD-fed *Ldlr*$^{-/-}$ mice. We also performed a lipidomics study to specifically assess the impact of amlexanox treatment, and demonstrated changes in the distribution of fatty acid species in the serum. Although amlexanox did not affect circulating levels of total fatty acids or saturated fatty acids, it mildly increased the levels of unsaturated fatty acids (Supplementary Figure 2A-2C). Among the saturated fatty acids, amlexanox increased the levels 17:0, 18:0, 20:0, while reducing 12:0, 14:0, 22:0, 23:0, 24:0, and 26:0 (Supplementary Figure 2D). Among the unsaturated fatty acids, amlexanox upregulated the levels of 18:2, 18:3 N3, 18:3 N6, 20:2, 20:5, 22:4, 22:5 N6, while down-regulating the levels of 16:1, 17:1, 18:1, 20:1, 20:3 N3, 20:4, 22:5 N3, 22:6, and 24:1 (Supplementary Figure 2E). Together, these data demonstrated that amlexanox markedly improved dyslipidemia in WD-fed *Ldlr*$^{-/-}$ mice.

Amlexanox increases bile acid synthesis and cholesterol excretion.

Our previous study demonstrated that amlexanox significantly increases energy expenditure to improve obesity and hypertriglyceridemia (30). To elucidate the mechanism by which amlexanox ameliorates hypercholesterolemia in WD-fed *Ldlr*$^{-/-}$ mice, we systematically examined cholesterol metabolism. Mice

were fed WD for 8 weeks with 4 additional weeks of feeding along with vehicle or amlexanox administration. 4 weeks of amlexanox treatment significantly reduced circulating levels of cholesterol and triglyceride in WD-fed *Ldlr*$^{-/-}$ mice (Figure 2A-2B). We assessed the rate of cholesterol absorption by assaying serum ^{14}C radioactivity 2 hrs after gavage of cold cholesterol mixed with ^{14}C-cholesterol. These data demonstrated that amlexanox did not affect cholesterol absorption (Figure 2C). Because liver is the major site of cholesterol synthesis, we also examined hepatic cholesterol synthesis rate in response to amlexanox administration. Mice gavaged with vehicle or amlexanox were injected with ^{3}H-acetate, and ^{3}H radioactivity in the liver sterol fraction was determined after 2hrs. Our results demonstrated that amlexanox did not affect radioactivity in the liver sterol fraction (Figure 2D), indicating no effect on cholesterol synthesis.

Given that amlexanox does not affect cholesterol absorption or synthesis, we examined whether the drug might control cholesterol excretion to attenuate hypercholesterolemia. WD-fed *Ldlr*$^{-/-}$ mice received vehicle or amlexanox, followed by oral gavage with cold cholesterol mixed with ^{14}C-cholesterol. After 21hrs, radioactivity was measured in serum, feces and liver lysates. Interestingly, radioactivity in serum was significantly reduced in mice gavaged with amlexanox, but significantly increased in the liver lysates, bile, and feces, indicating a dramatic increase in cholesterol clearance (Figure 2E-2H).

To understand the mechanism by which amlexanox increases cholesterol excretion, we performed RNA-seq on liver tissue of vehicle or amlexanox-treated mice. Our data revealed that amlexanox induced profound transcriptional changes in the livers of WD-fed *Ldlr*$^{-/-}$ mice (Figure 2I, Supplementary Figure 3A). Ontological analysis of genes upregulated by amlexanox showed significant enrichment of pathways that mediate bile acid synthesis and metabolism (Figure 2J). A notable example is the higher expression of Cyp7a1, the rate-limiting enzyme of bile acid synthesis (Figure 2K). Amlexanox also upregulated the expression of genes involved in fatty acid metabolism, while downregulating the expression of inflammation genes (Supplementary Figure 3B-3C).

Cholesterol is mainly excreted in the form of bile acids. To ascertain whether amlexanox affects bile acid synthesis and excretion, we measured bile acid levels in the feces of mice gavaged with vehicle or amlexanox. Amlexanox significantly increased the amount of fecal bile acids (Figure 2L). Together, these data suggest that inhibition of the protein kinases TBK1 and IKKε by amlexanox upregulates bile acid production to increase cholesterol excretion, and thus ameliorates hypercholesterolemia.

Amlexanox reduces circulating monocytes and lesion macrophage.

Inflammation is a major pathogenic factor for atherosclerosis. Under atherosclerotic conditions, macrophages infiltrate into the blood vessel wall and promote the formation of the necrotic core, which is a defining feature of unstable plaques (38). Staining of plaques with the macrophage marker macrophage antigen-3 (Mac-3) showed a significant attenuation of macrophage in aortic lesions (Figure 3A). To understand the underlying mechanism, we did a complete blood count to evaluate circulating immune cells. Interestingly, we found that amlexanox significantly reduced the number of monocytes and eosinophils, while neutrophil, lymphocyte, and basophil numbers were unaffected (Figure 3B-3F). Circulating monocytes are the major source of infiltrated macrophages, and monocytosis has been linked to atherosclerosis (38). These data indicate that amlexanox attenuates monocytosis, which in turn would lead to decreased numbers of monocytes recruited to the artery wall, contributing to the decrease of atherosclerosis. In contrast, amlexanox had no effect on the number of blood monocytes in mice fed normal chow diet (Supplementary Figure 4). We note that amlexanox was originally developed as an asthma treatment (39). Since eosinophilia is a major pathogenic factor in the development of asthma, the anti-eosinophilic effects of the drug might provide insight into the mechanism of amlexanox's anti-asthma function.

Amlexanox protects against vascular dysfunction *in vitro* and *in vivo*.

Vascular dysfunction is a major contributor to the pathogenesis of atherosclerosis (40-43). Endothelial cells that are dysregulated in atherosclerosis trigger monocyte adhesion, and thus promote macrophage

infiltration into the aortic vessel (3,4,41-43). Increased proliferation and migration of smooth muscle cells (SMCs) is also an indispensable component of plaque formation (44,45). To understand whether amlexanox affects monocyte-endothelial cell adhesion, we labeled THP-1 monocytes with the radiometric pH indicator BCECF, and treated human aortic endothelial cells (HAECs) with vehicle or TNFα. After removal of BCECF and TNFα, monocytes were incubated with HAECs. Non-adherent monocytes were washed away, and monocytes adhering to endothelial cells were visualized by fluorescence microscopy. As expected, TNFα increased monocyte-endothelial cell adhesion (Figure 4A-4B). Gene expression analysis on the HAECs demonstrated that TNFα and serum from WD-fed *Ldlr*$^{-/-}$ mice induced the expression of the inflammatory markers *Ccl2* and *Vcam1* in endothelial cells. These effects were significantly attenuated by the pretreatment of cells with amlexanox (Figure 4D-4D). The data suggested that amlexanox downregulated the TNFα-dependent expression of *Ccl2* and *Vcam1* in endothelial cells to attenuate monocyte adhesion.

To elucidate the site of amlexanox action, we determined whether amlexanox affects the function of smooth muscle cells (SMCs) to prevent plaque formation, performing a BrdU labeling assay on mouse vascular smooth muscle cells (MOVAS). Our data demonstrated that platelet-derived growth factor BB (PDGF-BB) significantly induced SMC proliferation. This effect was substantially inhibited by the pretreatment of cells with amlexanox (Figure 4E). We also utilized a Transwell cell migration assay to study amlexanox's effect on SMC migration. Amlexanox significantly reduced the migration of SMCs induced by the addition of serum from WD-fed *Ldlr*$^{-/-}$ mice (Figure 4F). Together, these findings demonstrate that amlexanox attenuates the proliferation and migration of smooth muscle cells, which could contribute to the amelioration of atherogenesis.

To elucidate the underlying mechanism by which amlexanox prevents cardiovascular dysfunction to protect against atherosclerosis, we dissected the aorta from WD-fed *Ldlr*$^{-/-}$ mice gavaged with vehicle or amlexanox and performed RNA-seq analysis on whole aorta. We observed 157 genes with levels of

expression in aorta of amlexanox-treated mice that are at least 1.5-folder less than the vehicle-treated aorta at an FDR of 0.05 and TMP greater than 16 (Figure 5A, Supplementary Figure 5A). Ontological analysis of genes downregulated by amlexanox demonstrated significant functional enrichment of atherogenic related categories, such as inflammatory response, cell chemotaxis, smooth muscle cell proliferation, and cell migration (Figure 5B). The expression of genes involved in inflammation and smooth muscle cell proliferation and migration are shown in Figure 5C-5D. Gene set enrichment analysis for differentially expressed transcripts in aorta revealed a significant downregulation of the inflammatory response, TNFα signaling, TGF signaling, and apoptotic pathways by amlexanox (Figure 5E, Supplementary Figure 5B). α-SMA (alpha-smooth muscle actin) staining showed a significant reduction of smooth muscle cells within the aortic lesions (Figure 5F), confirming that amlexanox attenuated SMC migration into plaques.

Discussion

Atherosclerosis and its complications, like heart attack and stroke, are the leading causes of death in modern society (2,3). Atherogenesis results from hypercholesterolemia (46,47), systemic chronic inflammation (3,48,49), and aortic cell dysfunctions (40-43,50), conditions that often appear together in cardiovascular disease patients. In this study, we found that amlexanox improves all three aspects of this syndrome to prevent atherosclerosis. Hypercholesterolemia, especially high blood concentrations of VLDL and LDL cholesterol, is essential for the development of aortic plaques (46). We showed that amlexanox significantly improved dyslipidemia and reduced both VLDL-cholesterol and LDL-cholesterol in WD-fed *Ldlr*$^{-/-}$ mice. Chronic inflammation is characterized by penetration of monocytes into aortic vessels, and monocyte-derived macrophages form the necrotic core of atherosclerotic lesions (3,51). Infiltration of monocytes/macrophages modulates the development of lesions, and affects their stability through cytokine secretion and cross-talk with artery wall cells (5). Oral gavage of amlexanox significantly reduced circulating monocytes as well as macrophage in aortic lesions. Additionally,

endothelial cell dysfunction results in an up-regulation of pro-inflammatory cytokines and adhesion molecules, which further increase monocyte adhesion (4). The phenotypic switch of smooth muscle cells from “contractile” to “synthetic” increases the proliferation of these cells (44). Increased expression of matrix metalloproteinases (MMPs) in aortic vessels cells results in extracellular matrix (ECM) remodeling, which promotes SMC migration into lesions (45). Our study demonstrated that amlexanox not only attenuates monocyte-endothelial adhesion, but also reduces SMC proliferation and migration to ameliorate the dysfunction of aortic vessel cells. Taken together, amlexanox improves all three aspects of this syndrome to protect against atherogenesis.

To understand the mechanism by which amlexanox improves these pathogenic aspects during atherogenesis, we profiled the transcriptome in liver and aorta. Bioinformatic analyses indicated that amlexanox significantly increased the expression of genes mediating bile acid synthesis in the liver, while attenuating the expression of inflammatory genes and the genes involving smooth muscle cell proliferation and migration. Our previous study demonstrated that amlexanox inhibits IKKε/TBK1 to attenuate inflammation (30,35). Here, we showed that amlexanox significantly reduced the expression of inflammation genes in the liver. Given that inflammation, especially via the production of TNFα, could repress the expression of *Cyp7a1* (52,53), we speculate that the improvement of systemic inflammation in WD-fed *Ldlr*$^{-/-}$ mice is responsible for the increased expression of bile acid synthesis genes. A recent study showed that amlexanox inhibits IKKε/TBK1 to repress TGFβ production (54). Consistent with this work, we found that amlexanox downregulated TGFβ signaling in aorta, which could result in the attenuation of smooth muscle cell proliferation and migration.

While current anti-atherosclerosis drugs are effective, their use is limited in certain populations. Most patients with metabolic syndrome present with hypercholesterolemia, hyperglycemia and insulin resistance. Although the use of statins in these population reduces the risk of CVD, their use maybe associated with the risk of a drug-induced increase in blood glucose, potentially exaggerating diabetes in

certain patients (14-16). Therefore, there is a need for new anti-atherosclerotic medications for a subgroup of patients with metabolic syndrome. Our previous studies showed that amlexanox significantly improves insulin sensitivity and glucose metabolism, while reducing hepatic steatosis in obese mice (30,33,34). A proof-of-concept clinical study also demonstrated that 12 weeks of amlexanox treatment was safe, and significantly decreased HbA1c levels, an effect that was more pronounced in a subset of patients with high systemic inflammation at baseline (35). The profound effects of the drug prompted us to evaluate amlexanox in a mouse model of atherosclerosis. Our findings demonstrate that amlexanox substantially attenuates diet-induced hypercholesterolemia and reduced aortic lesion area. Mechanistic studies suggest that amlexanox increases cholesterol excretion, prevents monocytosis, and attenuates aortic vessel cell dysfunction, indicating that amlexanox may represent a novel approach to the treatment of hypercholesterolemia and atherosclerosis in statin-resistant or metabolic syndrome patients with hyperglycemia, dyslipidemia and fatty liver diseases. More importantly, these data illustrate a potentially important role for the amlexanox targets, IKKε and TBK1, as a driver of cardiovascular disease.

Methods

Mice

Mice were used in accordance with the Guide for Care and Use of Laboratory Animals of the National Institute of Health. Mice were housed in a specific pathogen-free facility with a 12-h light, 12-h dark cycle, and given free access to food and water, except for fasting period. At 8 weeks of age, 18-20g male *Ldlr*$^{-/-}$ mice (The Jackson Laboratory, #002207) were matched for age, body weight and total cholesterol and placed on a Western diet (WD) (Research Diets, D12079Bi). Mouse were orally gavaged 25mg/kg amlexanox (Abcam, Cat. ab142825) or vehicle every other day with the continuation of WD feeding. During the feeding, mice were weighed monthly. At sacrifice, tissues were weighed. Blood samples were collected. Complete blood count was done by hematology core at UCSD. Liver H&E staining was carried

out by UCSD histology core. Stained tissue was visualized with NanoZoomer Slide Scanner at UCSD School of Medicine microscopy core. Lipidomic study was performed at UCSD lipidomics core.

Atherosclerotic plaque analysis

The aortas were dissected under a microscope and fixed in 4% formalin–sucrose, opened, flattened pinned and stained with Sudan IV, and images of the aortas were captured and quantified by analysis of the entire en face aorta as previously described (55). Aortic root cross-sectional lesion areas were quantified using serial cross-sections taken at 100μm intervals between 100μm and 900μm beginning with the first appearance of the first leaflet of the aortic valve until the last leaflet. Mean lesion size at each 100μm section in each animal was determined by computer-assisted morphometry on serial 10μm paraffin sections. Modified van Gieson elastic stain was used to enhance the contrast between the intima and surrounding tissue. Cross-sectional plaque area and plaque morphology were evaluated blindly. The results are presented as mean of all values for each interval plotted versus the distance from first leaflet and the overall extent of aortic root lesions was determined by area under the curve (AUC) analysis of all serial sections in each group. Mac-3 staining on aortic roots was performed using anti-Mac-3 antibody (Santa Cruz, Cat. sc-20004).

Cholesterol Metabolism

WD-fed *Ldlr*$^{-/-}$ mice were fasted overnight, and then intraperitoneally injected with 10mCi/kg ^{3}H-acetate. After 2hrs, ^{3}H activity in liver sterol fraction was measured to indicate cholesterol synthesis rate. WD-fed *Ldlr*$^{-/-}$ mice were fasted overnight, and then orally gavaged a mixture of 2mg/kg cholesterol and 20μCi/kg ^{14}C-cholesterol. After 2hrs, serum ^{14}C activity was examined as an indication of cholesterol absorption rate. After 21hrs, ^{14}C activities in serum, liver lysate, bile, and feces were measured to examine cholesterol excretion.

Lipid measurement

Blood/Tissue triglyceride and cholesterol levels were determined using the Triglyceride Quantification Colorimetric/Fluorometric Kit (Biovision, Cat. K622) and total Cholesterol and Cholesterol Ester Colorimetric/Fluorometric Kit (Biovision, Cat. K603) according to the manufacturer's instruction respectively. All values were analyzed from 12 hours fasted mice.

Lipoprotein profiling was performed on terminal blood samples from a pool of 5 mice using fast performance liquid chromatography equipped with a Superose 6 column, and total cholesterol and triglycerides levels in each fraction were determined as described above.

Fecal bile acid measurement

Feces were weighed out. Bile acids were extract using 90% ethanol with 0.1N NaOH. Bile acids were determined using Mouse Total Bile Acids Assay Kit (Crystalchem, Cat. 80471) according to the manufacturer's instruction.

Gene expression analysis

Analysis of gene expression was performed as previously described (56,57). Tissues were homogenized in TRIzol Reagent (Life Technologies). RNA was isolated with PureLink RNA mini kit (Life Technologies). 1µg of purified RNA was used for reverse transcription-PCR to generate cDNA using High-Capacity cDNA Reverse Transcription Kit (Applied Biosystem). ΔΔCt real time PCR with Power SYBR Green PCR Master Mix (Life Technologies) and QuantStudio 5 Real-Time PCR System were used to analyze cDNA. *Ppia* (Cyclophilin A) was used as endogenous control. The following primers were used for qPCR. *Ccl2* Forward: CAGCCAGATGCAATCAATGCC; Reverse: TGGAATCCTGAACCCACTTCT. *Ppia* Forward: GGCAAATGCTGGACCCAACACA; Reverse: TGCTGGTCTTGCCATTCCTGGA. *Vcam1* Forward: CCGGATTGCTGCTCAGATTGGA; Reverse: AGCGTGGAATTGGTCCCCTCA.

Cell migration assay

Mouse vascular smooth muscle cells (MOVAS) (ATCC, Cat. CRL-2797) were cultured within the Transwells. Cells were treated with PDGF-BB or serum in the presence of vehicle or amlexanox for 24hrs. MOVAS that migrate to the lower side of Transwells were stained with 0.1% Crystal Violet and visualized by brightfield microscropy. Crystal Violet was eluted by 10% acetic acid. Absorbance was measured at 590nm for quantification.

Cell adhesion assay

Human aortic endothelial cells (HAECs) (ATCC, Cat. PCS-100-011) were treated with TNFα or serum for 10hrs in the presence of vehicle or 100μM amlexanox. THP-1 cells were incubated with 5μM (BCECF, AM) for 30min. Both cells will be washed with PBS for 3 times. THP-1 cells were transferred and co-cultured with HAECs for 30min. Non-adherent monocytes were washed away. Monocytes that adhere to endothelial cells were visualized by florescence microscopy.

BrdU cell proliferation assay

Mouse vascular smooth muscle cells (MOVAS) were cultured in 24-well cell culture plate and treated with PDGF-BB in the presence of vehicle or 100μM amlexanox for 24hrs. Cell proliferation rate was determined using BrdU Cell Proliferation Assay Kit (Biovision, Cat. K306) according to the manufacturer's instruction.

RNA-Seq Library Preparation

Total RNA was isolated from mice livers homogenized with TRIzol reagent and purified using Quick RNA mini prep columns and RNase-free DNase digestion according to the manufacturer's instructions (Life Technologies). RNA quality was assessed by an Agilent 2100 Bioanalyzer. Sequencing libraries were prepared in biological replicates from polyA enriched mRNA. RNA-seq libraries were prepared from poly(A)-enriched mRNA as previously described (58). Total RNA-seq library was prepared by UCSD IGM Core using Illumina Total RNA prep kit. Libraries were quantified using a Qubit dsDNA HS Assay

Kit (Thermo Fisher Scientific) and sequenced on a Hiseq 4000 (Illumina, San Diego, CA) according to the manufacturer's instructions.

RNA-Seq Analysis

RNA-seq analysis was conducted as previously described (59,60). FASTQ files from sequencing experiments were mapped to the mouse mm10 genome. STAR with default parameters was used to map RNA-seq experiments (61). To compare differential gene expression between indicated groups, HOMER's analyzeRepeats with the option rna and the parameters -condenseGenes, -noadj, and -count exons was used on two-three replicates per condition (62). Each sequencing experiment was normalized to a total of 107 uniquely mapped tags by adjusting the number of tags at each position in the genome to the correct fractional amount given the total tags mapped. Sequence experiments were visualized by preparing custom tracks for the UCSC genome browser. Differential gene expression was assessed with DESeq2 using HOMER's getDiffExpression.pl with the parameters -P-adj 0.05 and -log2 fold 0.585 (for 1.5-fold differently expressed genes) (63). For all genes the TPM (transcript per kilobase million) values were plotted and colored according to fold change. For various ontology analyses, either HOMER or Metascape was used (64). The accession number for the transcriptomic data reported in this paper is GEO: GSE209621.

Statistics

All data in animal studies are shown as mean ± SEM., while data from in vitro studies are shown as mean ± SD. Replicates are indicated in figure legends. N represents the number of experimental replicates. F-test was performed to determine the equality of variance. When comparing two groups, statistical analysis was performed using a two-tailed Student's t-test, except when the f-test suggested that variances are statistically different. For analysis of more than two groups, we used analysis of variance (ANOVA) to determine equality of variance. Comparisons between groups were performed with Tukey-Krammer post-hoc analysis. For all tests, $P<0.05$ was considered statistically significant (56).

Study approval

The animal studies were approved by the Institutional Animal Care and Use Committee of (IACUC) of UCSD and UTHSCSA.

Author Contributions

P.Z. and X.S. conceptualized and designed the study. A.R.S. and J.L.W. supervised the study. P.Z., X.S., Z.L., H.Y. performed experiments. P.Z., X.S., Z.L., D.L., Z.S. analyzed data. C.K.G. provided support on atherosclerosis and next generation sequencing. P.Z. and X.S. wrote the manuscript. A.R.S., J.L.W. edited the manuscript.

Acknowledgements

We thank the UCSD histology core for tissue sectioning and H&E staining. We thank Jennifer Pattison and Karen Bowden for Morphological study on atherosclerotic lesions. We thank Qiongyu Chen and the hematology core for hematological analysis. IHC images were taken at UCSD School of Medicine microscopy core (supported by NINDS P30NS047101). We thank Oswald Quehenberger and the lipidomics core for lipidomic analysis. This work was supported by NIH K99/R00HL143277, R01DK133304, CPRIT RR200089 to P.Z.; NIH K99/R00HL148504, CPRIT RR210005 to X.S.; NIH P30DK063491, R01DK124496, R01DK117551, R01DK125820, R01DK122804 to A.R.S.; and P01HL147835 to J.L.W..

Competing interests

A.R.S. and P.Z. are named inventors on an invention disclosure for the use of amlexanox to treat cardiovascular disease. A.R.S. is a named inventor on patents pertaining to the use of amlexanox and its analogs for the treatment of metabolic diseases. A.R.S. is a founder of Elgia Therapeutics. J.L.W. is a founding member of Oxitope, Inc. The other authors declare that they have no competing interests.

References

1. O'Neill, S., and O'Driscoll, L. (2015) Metabolic syndrome: a closer look at the growing epidemic and its associated pathologies. *Obes Rev* **16**, 1-12
2. Glass, C. K., and Witztum, J. L. (2001) Atherosclerosis. the road ahead. *Cell* **104**, 503-516
3. Lusis, A. J. (2000) Atherosclerosis. *Nature* **407**, 233-241
4. Mestas, J., and Ley, K. (2008) Monocyte-endothelial cell interactions in the development of atherosclerosis. *Trends Cardiovasc Med* **18**, 228-232
5. Moore, K. J., Sheedy, F. J., and Fisher, E. A. (2013) Macrophages in atherosclerosis: a dynamic balance. *Nat Rev Immunol* **13**, 709-721
6. Moore, K. J., and Tabas, I. (2011) Macrophages in the pathogenesis of atherosclerosis. *Cell* **145**, 341-355
7. Gould, A. L., Rossouw, J. E., Santanello, N. C., Heyse, J. F., and Furberg, C. D. (1998) Cholesterol reduction yields clinical benefit: impact of statin trials. *Circulation* **97**, 946-952
8. Schartl, M., Bocksch, W., Koschyk, D. H., Voelker, W., Karsch, K. R., Kreuzer, J., Hausmann, D., Beckmann, S., and Gross, M. (2001) Use of intravascular ultrasound to compare effects of different strategies of lipid-lowering therapy on plaque volume and composition in patients with coronary artery disease. *Circulation* **104**, 387-392
9. Tobert, J. A., Bell, G. D., Birtwell, J., James, I., Kukovetz, W. R., Pryor, J. S., Buntinx, A., Holmes, I. B., Chao, Y. S., and Bolognese, J. A. (1982) Cholesterol-lowering effect of mevinolin, an inhibitor of 3-hydroxy-3-methylglutaryl-coenzyme a reductase, in healthy volunteers. *J Clin Invest* **69**, 913-919

10. Tobert, J. A., Hitzenberger, G., Kukovetz, W. R., Holmes, I. B., and Jones, K. H. (1982) Rapid and substantial lowering of human serum cholesterol by mevinolin (MK-803), an inhibitor of hydroxymethylglutaryl-coenzyme A reductase. *Atherosclerosis* **41**, 61-65

11. Avogaro, P., Bittolo-Bon, G., Pais, M., and Taroni, G. C. (1977) Effect of a new niacin derivative (nicotinic hexaester of D-glucitol) on type IIA, IIB and IV hyperlipoproteinemia in man. *Pharmacol Res Commun* **9**, 599-606

12. Kane, J. P., Malloy, M. J., Tun, P., Phillips, N. R., Freedman, D. D., Williams, M. L., Rowe, J. S., and Havel, R. J. (1981) Normalization of low-density-lipoprotein levels in heterozygous familial hypercholesterolemia with a combined drug regimen. *N Engl J Med* **304**, 251-258

13. Mantell, G. (1989) Lipid lowering drugs in atherosclerosis--the HMG-CoA reductase inhibitors. *Clin Exp Hypertens A* **11**, 927-941

14. Heemskerk, M. M., van den Berg, S. A., Pronk, A. C., van Klinken, J. B., Boon, M. R., Havekes, L. M., Rensen, P. C., van Dijk, K. W., and van Harmelen, V. (2014) Long-term niacin treatment induces insulin resistance and adrenergic responsiveness in adipocytes by adaptive downregulation of phosphodiesterase 3B. *Am J Physiol Endocrinol Metab* **306**, E808-813

15. Kain, V., Kapadia, B., Misra, P., and Saxena, U. (2015) Simvastatin may induce insulin resistance through a novel fatty acid mediated cholesterol independent mechanism. *Sci Rep* **5**, 13823

16. Mitchell, P., and Marette, A. (2014) Statin-induced insulin resistance through inflammasome activation: sailing between Scylla and Charybdis. *Diabetes* **63**, 3569-3571

17. LaRosa, J. (1989) Review of clinical studies of bile acid sequestrants for lowering plasma lipid levels. *Cardiology* **76 Suppl 1**, 55-61; discussion 61-54

18. Weintraub, M. S., Grosskopf, I., Charach, G., Mor, R., Rubinstein, A., Wollman, Y., Judevices, R., and Iaina, A. (1995) Bezafibrate therapy in patients with isolated low high-density lipoprotein cholesterol levels may have a beneficial effect in prevention of atherosclerosis. *Metabolism* **44**, 1401-1409

19. West, A. M., Anderson, J. D., Meyer, C. H., Epstein, F. H., Wang, H., Hagspiel, K. D., Berr, S. S., Harthun, N. L., DiMaria, J. M., Hunter, J. R., Christopher, J. M., Chew, J. D., Winberry, G. B., and Kramer, C. M. (2011) The effect of ezetimibe on peripheral arterial atherosclerosis depends upon statin use at baseline. *Atherosclerosis* **218**, 156-162

20. Nissen, S. E., Dent-Acosta, R. E., Rosenson, R. S., Stroes, E., Sattar, N., Preiss, D., Mancini, G. B., Ballantyne, C. M., Catapano, A., Gouni-Berthold, I., Stein, E. A., Xue, A., Wasserman, S. M., Scott, R., Thompson, P. D., and Investigators, G.-. (2016) Comparison of PCSK9 Inhibitor Evolocumab vs Ezetimibe in Statin-Intolerant Patients: Design of the Goal Achievement After Utilizing an Anti-PCSK9 Antibody in Statin-Intolerant Subjects 3 (GAUSS-3) Trial. *Clin Cardiol* **39**, 137-144

21. Stein, E. A., Gipe, D., Bergeron, J., Gaudet, D., Weiss, R., Dufour, R., Wu, R., and Pordy, R. (2012) Effect of a monoclonal antibody to PCSK9, REGN727/SAR236553, to reduce low-density lipoprotein cholesterol in patients with heterozygous familial hypercholesterolaemia on stable statin dose with or without ezetimibe therapy: a phase 2 randomised controlled trial. *Lancet* **380**, 29-36

22. Stein, E. A., Mellis, S., Yancopoulos, G. D., Stahl, N., Logan, D., Smith, W. B., Lisbon, E., Gutierrez, M., Webb, C., Wu, R., Du, Y., Kranz, T., Gasparino, E., and Swergold, G. D. (2012) Effect of a monoclonal antibody to PCSK9 on LDL cholesterol. *N Engl J Med* **366**, 1108-1118

23. Park, E. J., Lee, J. H., Yu, G. Y., He, G., Ali, S. R., Holzer, R. G., Osterreicher, C. H., Takahashi, H., and Karin, M. (2010) Dietary and genetic obesity promote liver inflammation and tumorigenesis by enhancing IL-6 and TNF expression. *Cell* **140**, 197-208

24. Weisberg, S. P., McCann, D., Desai, M., Rosenbaum, M., Leibel, R. L., and Ferrante, A. W., Jr. (2003) Obesity is associated with macrophage accumulation in adipose tissue. *J Clin Invest* **112**, 1796-1808

25. Xu, H., Barnes, G. T., Yang, Q., Tan, G., Yang, D., Chou, C. J., Sole, J., Nichols, A., Ross, J. S., Tartaglia, L. A., and Chen, H. (2003) Chronic inflammation in fat plays a crucial role in the development of obesity-related insulin resistance. *J Clin Invest* **112**, 1821-1830

26. Arkan, M. C., Hevener, A. L., Greten, F. R., Maeda, S., Li, Z. W., Long, J. M., Wynshaw-Boris, A., Poli, G., Olefsky, J., and Karin, M. (2005) IKK-beta links inflammation to obesity-induced insulin resistance. *Nat Med* **11**, 191-198

27. Baker, R. G., Hayden, M. S., and Ghosh, S. (2011) NF-kappaB, inflammation, and metabolic disease. *Cell Metab* **13**, 11-22

28. Chiang, S. H., Bazuine, M., Lumeng, C. N., Geletka, L. M., Mowers, J., White, N. M., Ma, J. T., Zhou, J., Qi, N., Westcott, D., Delproposto, J. B., Blackwell, T. S., Yull, F. E., and Saltiel, A. R. (2009) The protein kinase IKKepsilon regulates energy balance in obese mice. *Cell* **138**, 961-975

29. Pamukcu, B., Lip, G. Y., and Shantsila, E. (2011) The nuclear factor--kappa B pathway in atherosclerosis: a potential therapeutic target for atherothrombotic vascular disease. *Thromb Res* **128**, 117-123

30. Reilly, S. M., Chiang, S. H., Decker, S. J., Chang, L., Uhm, M., Larsen, M. J., Rubin, J. R., Mowers, J., White, N. M., Hochberg, I., Downes, M., Yu, R. T., Liddle, C., Evans, R. M., Oh, D., Li, P., Olefsky, J. M., and Saltiel, A. R. (2013) An inhibitor of the protein kinases TBK1 and IKK-varepsilon improves obesity-related metabolic dysfunctions in mice. *Nat Med* **19**, 313-321

31. Imokawa, S., Satou, A., Taniguchi, M., Toyoshima, M., Nakazawa, K., Hayakawa, H., and Chida, K. (1993) [Amlexanox has an acute bronchodilator effect in patients with aspirin-induced asthma (AIA)]. *Nihon Kyobu Shikkan Gakkai Zasshi* **31**, 976-982

32. Takenaka, H., Shoji, H., Mizukoshi, F., Kushumi, T., Matsumoto, T., and Kuriki, H. (1988) [Effects of AA-673 on antigen-induced histamine release from leukocytes in patients with allergic rhinitis]. *Arerugi* **37**, 1094-1100

33. Huh, J. Y., Reilly, S. M., Abu-Odeh, M., Murphy, A. N., Mahata, S. K., Zhang, J., Cho, Y., Seo, J. B., Hung, C. W., Green, C. R., Metallo, C. M., and Saltiel, A. R. (2020) TANK-Binding Kinase 1 Regulates the Localization of Acyl-CoA Synthetase ACSL1 to Control Hepatic Fatty Acid Oxidation. *Cell Metab* **32**, 1012-1027 e1017

34. Zhao, P., and Saltiel, A. R. (2020) Interaction of Adipocyte Metabolic and Immune Functions Through TBK1. *Front Immunol* **11**, 592949

35. Oral, E. A., Reilly, S. M., Gomez, A. V., Meral, R., Butz, L., Ajluni, N., Chenevert, T. L., Korytnaya, E., Neidert, A. H., Hench, R., Rus, D., Horowitz, J. F., Poirier, B., Zhao, P., Lehmann, K., Jain, M., Yu, R., Liddle, C., Ahmadian, M., Downes, M., Evans, R. M., and Saltiel, A. R. (2017) Inhibition of IKKvarepsilon and TBK1 Improves Glucose Control in a Subset of Patients with Type 2 Diabetes. *Cell Metab* **26**, 157-170 e157

36. Mowers, J., Uhm, M., Reilly, S. M., Simon, J., Leto, D., Chiang, S. H., Chang, L., and Saltiel, A. R. (2013) Inflammation produces catecholamine resistance in obesity via activation of PDE3B by the protein kinases IKKepsilon and TBK1. *Elife* **2**, e01119

37. Reilly, S. M., Abu-Odeh, M., Ameka, M., DeLuca, J. H., Naber, M. C., Dadpey, B., Ebadat, N., Gomez, A. V., Peng, X., Poirier, B., Walk, E., Potthoff, M. J., and Saltiel, A. R. (2021) FGF21 is required for the metabolic benefits of IKKepsilon/TBK1 inhibition. *J Clin Invest* **131**

38. Ley, K., Miller, Y. I., and Hedrick, C. C. (2011) Monocyte and macrophage dynamics during atherogenesis. *Arterioscler Thromb Vasc Biol* **31**, 1506-1516

39. Dosanjh, A., and Won, C. Y. (2020) Amlexanox: A Novel Therapeutic for Atopic, Metabolic, and Inflammatory Disease. *Yale J Biol Med* **93**, 759-763

40. Bennett, M. R., Sinha, S., and Owens, G. K. (2016) Vascular Smooth Muscle Cells in Atherosclerosis. *Circ Res* **118**, 692-702

41. Gimbrone, M. A., Jr., and Garcia-Cardena, G. (2016) Endothelial Cell Dysfunction and the Pathobiology of Atherosclerosis. *Circ Res* **118**, 620-636

42. Hadi, H. A., Carr, C. S., and Al Suwaidi, J. (2005) Endothelial dysfunction: cardiovascular risk factors, therapy, and outcome. *Vasc Health Risk Manag* **1**, 183-198

43. Mudau, M., Genis, A., Lochner, A., and Strijdom, H. (2012) Endothelial dysfunction: the early predictor of atherosclerosis. *Cardiovasc J Afr* **23**, 222-231

44. Gomez, D., and Owens, G. K. (2012) Smooth muscle cell phenotypic switching in atherosclerosis. *Cardiovasc Res* **95**, 156-164

45. Newby, A. C. (2006) Matrix metalloproteinases regulate migration, proliferation, and death of vascular smooth muscle cells by degrading matrix and non-matrix substrates. *Cardiovasc Res* **69**, 614-624

46. Goldstein, J. L., and Brown, M. S. (1977) The low-density lipoprotein pathway and its relation to atherosclerosis. *Annu Rev Biochem* **46**, 897-930

47. Kottke, B. A., Pineda, A. A., Case, M. T., Orsuzar, A. M., and Brzys, K. A. (1988) Hypercholesterolemia and atherosclerosis: present and future therapy including LDL-apheresis. *J Clin Apher* **4**, 35-46

48. Libby, P. (2002) Inflammation in atherosclerosis. *Nature* **420**, 868-874

49. Libby, P. (2012) Inflammation in Atherosclerosis. *Arterioscl Throm Vas* **32**, 2045-2051

50. Rudijanto, A. (2007) The role of vascular smooth muscle cells on the pathogenesis of atherosclerosis. *Acta Med Indones* **39**, 86-93

51. Seimon, T., and Tabas, I. (2009) Mechanisms and consequences of macrophage apoptosis in atherosclerosis. *J Lipid Res* **50 Suppl**, S382-387

52. De Fabiani, E., Mitro, N., Anzulovich, A. C., Pinelli, A., Galli, G., and Crestani, M. (2001) The negative effects of bile acids and tumor necrosis factor-alpha on the transcription of cholesterol 7alpha-hydroxylase gene (CYP7A1) converge to hepatic nuclear factor-4: a novel mechanism of feedback regulation of bile acid synthesis mediated by nuclear receptors. *J Biol Chem* **276**, 30708-30716

53. Henkel, A. S., Anderson, K. A., Dewey, A. M., Kavesh, M. H., and Green, R. M. (2011) A chronic high-cholesterol diet paradoxically suppresses hepatic CYP7A1 expression in FVB/NJ mice. *J Lipid Res* **52**, 289-298

54. Zhou, Z., Qi, J., Zhao, J., Lim, C. W., Kim, J. W., and Kim, B. (2020) Dual TBK1/IKKvarepsilon inhibitor amlexanox attenuates the severity of hepatotoxin-induced liver fibrosis and biliary fibrosis in mice. *J Cell Mol Med* **24**, 1383-1398

55. Que, X., Hung, M. Y., Yeang, C., Gonen, A., Prohaska, T. A., Sun, X., Diehl, C., Maatta, A., Gaddis, D. E., Bowden, K., Pattison, J., MacDonald, J. G., Yla-Herttuala, S., Mellon, P. L., Hedrick, C. C., Ley, K., Miller, Y. I., Glass, C. K., Peterson, K. L., Binder, C. J., Tsimikas, S., and Witztum, J. L. (2018) Oxidized phospholipids are proinflammatory and proatherogenic in hypercholesterolaemic mice. *Nature* **558**, 301-306

56. Zhao, P., Wong, K. I., Sun, X. L., Reilly, S. M., Uhm, M., Liao, Z. J., Skorobogatko, Y., and Saltiel, A. R. (2018) TBK1 at the Crossroads of Inflammation and Energy Homeostasis in Adipose Tissue. *Cell* **172**, 731-743

57. Zhao, P., Sun, X., Chaggan, C., Liao, Z., In Wong, K., He, F., Singh, S., Loomba, R., Karin, M., Witztum, J. L., and Saltiel, A. R. (2020) An AMPK-caspase-6 axis controls liver damage in nonalcoholic steatohepatitis. *Science* **367**, 652-660

58. Oishi, Y., Spann, N. J., Link, V. M., Muse, E. D., Strid, T., Edillor, C., Kolar, M. J., Matsuzaka, T., Hayakawa, S., Tao, J., Kaikkonen, M. U., Carlin, A. F., Lam, M. T., Manabe, I., Shimano, H., Saghatelian, A., and Glass, C. K. (2017) SREBP1 Contributes to Resolution of Pro-inflammatory TLR4 Signaling by Reprogramming Fatty Acid Metabolism. *Cell Metab* **25**, 412-427

59. Link, V. M., Duttke, S. H., Chun, H. B., Holtman, I. R., Westin, E., Hoeksema, M. A., Abe, Y., Skola, D., Romanoski, C. E., Tao, J., Fonseca, G. J., Troutman, T. D., Spann, N. J., Strid, T., Sakai, M., Yu, M., Hu, R., Fang, R., Metzler, D., Ren, B., and Glass, C. K. (2018) Analysis of Genetically

Diverse Macrophages Reveals Local and Domain-wide Mechanisms that Control Transcription Factor Binding and Function. *Cell* **173**, 1796-1809 e1717

60. Sun, X., Seidman, J. S., Zhao, P., Troutman, T. D., Spann, N. J., Que, X., Zhou, F., Liao, Z., Pasillas, M., Yang, X., Magida, J. A., Kisseleva, T., Brenner, D. A., Downes, M., Evans, R. M., Saltiel, A. R., Tsimikas, S., Glass, C. K., and Witztum, J. L. (2020) Neutralization of Oxidized Phospholipids Ameliorates Non-alcoholic Steatohepatitis. *Cell Metab* **31**, 189-206 e188

61. Dobin, A., Davis, C. A., Schlesinger, F., Drenkow, J., Zaleski, C., Jha, S., Batut, P., Chaisson, M., and Gingeras, T. R. (2013) STAR: ultrafast universal RNA-seq aligner. *Bioinformatics* **29**, 15-21

62. Heinz, S., Benner, C., Spann, N., Bertolino, E., Lin, Y. C., Laslo, P., Cheng, J. X., Murre, C., Singh, H., and Glass, C. K. (2010) Simple combinations of lineage-determining transcription factors prime cis-regulatory elements required for macrophage and B cell identities. *Mol Cell* **38**, 576-589

63. Love, M. I., Huber, W., and Anders, S. (2014) Moderated estimation of fold change and dispersion for RNA-seq data with DESeq2. *Genome Biol* **15**, 550

64. Tripathi, S., Pohl, M. O., Zhou, Y., Rodriguez-Frandsen, A., Wang, G., Stein, D. A., Moulton, H. M., DeJesus, P., Che, J., Mulder, L. C., Yanguez, E., Andenmatten, D., Pache, L., Manicassamy, B., Albrecht, R. A., Gonzalez, M. G., Nguyen, Q., Brass, A., Elledge, S., White, M., Shapira, S., Hacohen, N., Karlas, A., Meyer, T. F., Shales, M., Gatorano, A., Johnson, J. R., Jang, G., Johnson, T., Verschueren, E., Sanders, D., Krogan, N., Shaw, M., Konig, R., Stertz, S., Garcia-Sastre, A., and Chanda, S. K. (2015) Meta- and Orthogonal Integration of Influenza "OMICs" Data Defines a Role for UBR4 in Virus Budding. *Cell Host Microbe* **18**, 723-735

Fig. 1

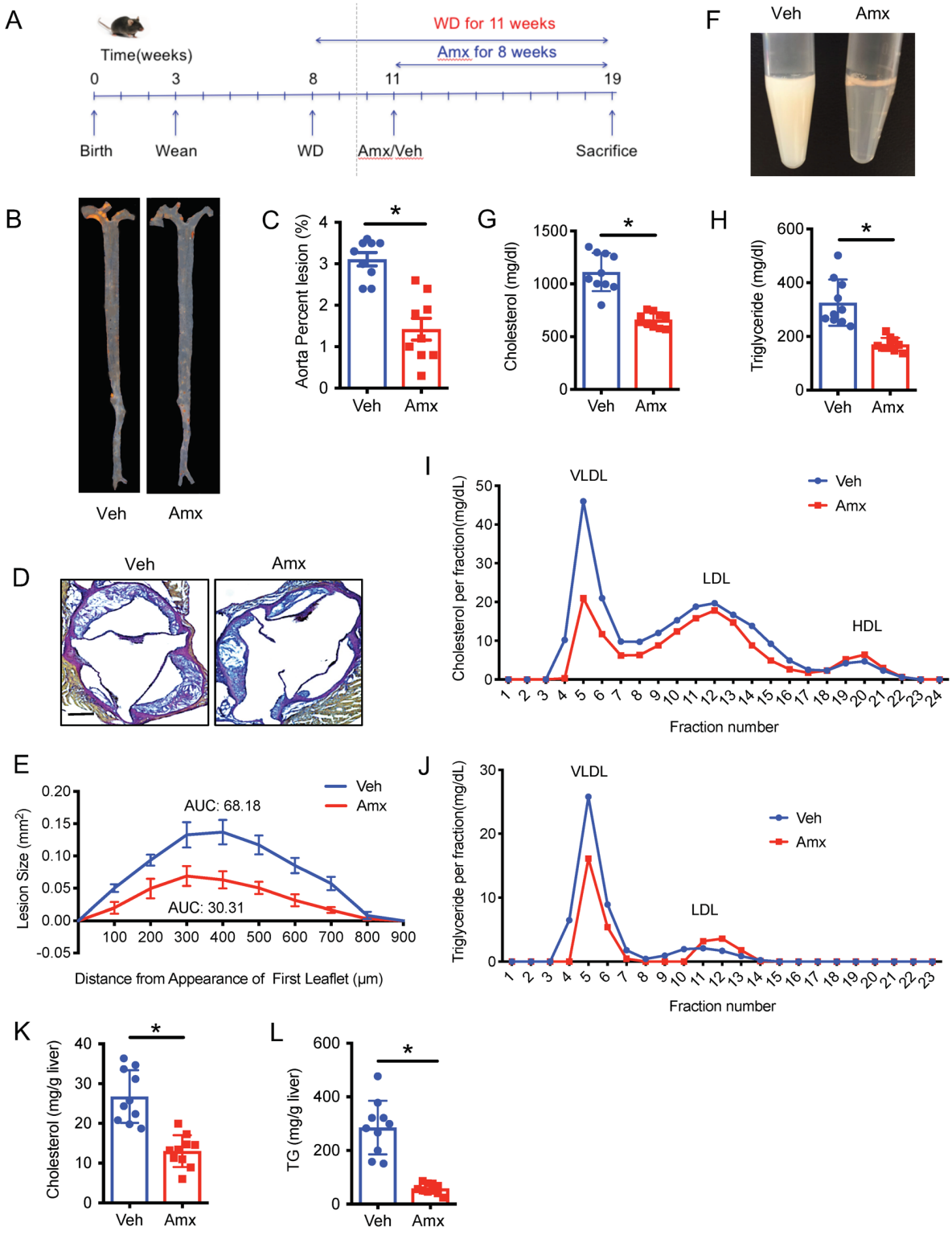
A
Time(weeks)
0
3
8
11
19
WD for 11 weeks
Amx for 8 weeks
Birth
Wean
WD
Amx/Veh
Sacrifice
F
Veh
Amx
B
Veh
Amx
C
Aorta Percent lesion (%)
Veh
Amx
G
Cholesterol (mg/dl)
H
Triglyceride (mg/dl)
D
Veh
Amx
I
VLDL
LDL
HDL
Veh
Amx
Cholesterol per fraction(mg/dL)
Fraction number
E
AUC: 68.18
AUC: 30.31
Lesion Size (mm²)
Distance from Appearance of First Leaflet (μm)
J
VLDL
LDL
Triglyceride per fraction(mg/dL)
Fraction number
K
Cholesterol (mg/g liver)
L
TG (mg/g liver)

Figure 1. Amlexanox improves dyslipidemia and protects against atherosclerosis. *Ldlr*$^{-/-}$ mice were fed WD for 3 weeks, then orally gavaged with vehicle or amlexanox (25mg/kg BW) for 8 weeks with the continuation of WD feeding. **A**. Schematic diagram of experimental design and mouse model. **B.** En face staining of aorta. **C.** Quantification of lesion areas in (B). **D.** Van Gieson elastic staining of aortic roots. **E.** Quantification of aortic roots staining in (D). **F**. Photo of serum from WD-fed *Ldlr*$^{-/-}$ mice treated with vehicle or amlexanox. **G.** Fasting serum cholesterol level. **H.** Fasting serum triglycerides level. **I, J**. Distribution of plasma cholesterol (I) and triglycerides(J) by fast performance liquid chromatography in pools of equal aliquots of plasma from vehicle or amlexanox-treated WD-fed *Ldlr*$^{-/-}$ mice (n=5). **K.** Hepatic cholesterol levels. **L**. Hepatic triglycerides levels. Mean ± SEM. *, $P<0.05$, Student's unpaired *t* test.

Fig. 2

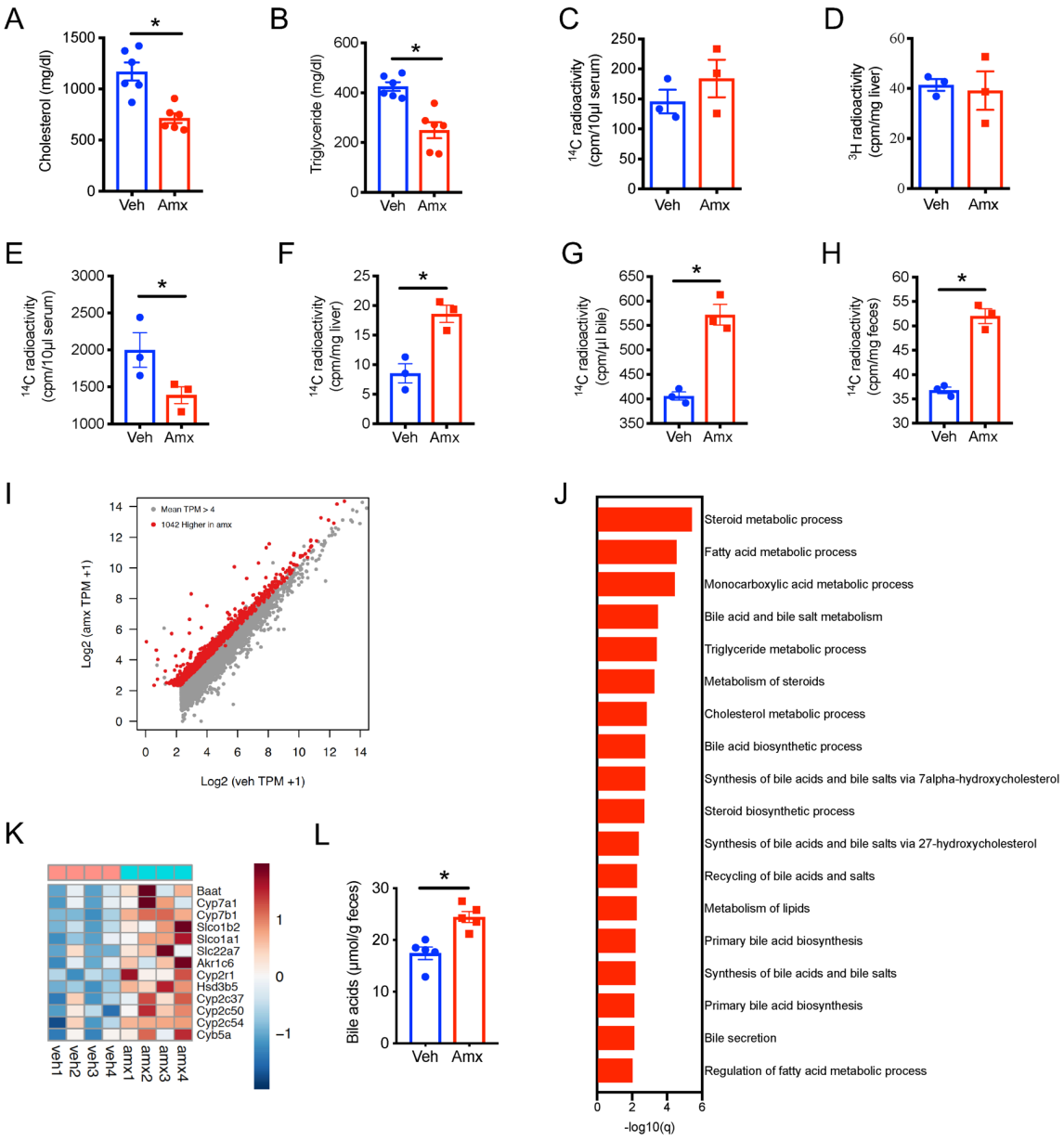
A
Cholesterol (mg/dl)
1500
1000
500
0
Veh
Amx
*
B
Triglyceride (mg/dl)
600
400
200
0
Veh
Amx
*
C
14C radioactivity (cpm/10µl serum)
250
200
150
100
50
0
Veh
Amx
D
3H radioactivity (cpm/mg liver)
60
40
20
0
Veh
Amx
E
14C radioactivity (cpm/10µl serum)
3000
2500
2000
1500
1000
Veh
Amx
*
F
14C radioactivity (cpm/mg liver)
25
20
15
10
5
0
Veh
Amx
*
G
14C radioactivity (cpm/µl bile)
650
600
550
500
450
400
350
Veh
Amx
*
H
14C radioactivity (cpm/mg feces)
60
55
50
45
40
35
30
Veh
Amx
*
I
Mean TPM > 4
1042 Higher in amx
Log2 (amx TPM +1)
Log2 (veh TPM +1)
0
2
4
6
8
10
12
14
J
Steroid metabolic process
Fatty acid metabolic process
Monocarboxylic acid metabolic process
Bile acid and bile salt metabolism
Triglyceride metabolic process
Metabolism of steroids
Cholesterol metabolic process
Bile acid biosynthetic process
Synthesis of bile acids and bile salts via 7alpha-hydroxycholesterol
Steroid biosynthetic process
Synthesis of bile acids and bile salts via 27-hydroxycholesterol
Recycling of bile acids and salts
Metabolism of lipids
Primary bile acid biosynthesis
Synthesis of bile acids and bile salts
Primary bile acid biosynthesis
Bile secretion
Regulation of fatty acid metabolic process
0
2
4
6
-log10(q)
K
Baat
Cyp7a1
Cyp7b1
Slco1b2
Slco1a1
Slc22a7
Akr1c6
Cyp2r1
Hsd3b5
Cyp2c37
Cyp2c50
Cyp2c54
Cyb5a
veh1
veh2
veh3
veh4
amx1
amx2
amx3
amx4
1
0
−1
L
Bile acids (µmol/g feces)
30
20
10
0
Veh
Amx
*

Figure 2. Amlexanox increases bile acid synthesis and cholesterol excretion. A-E. Cholesterol metabolism in *Ldlr*$^{-/-}$ mice fed WD for 8 weeks, then orally gavaged with vehicle or amlexanox for 4 weeks with the continuation of WD feeding. **A.** Fasting serum cholesterol. **B.** Fasting serum triglyceride. **C.** Serum ^{14}C activity 2hrs after gavage of a mixture of cholesterol and ^{14}C-cholesterol. **D.** ^{3}H activity in liver sterol fraction 2hrs after injection of ^{3}H-acetate. **E-H.** ^{14}C activity in serum (E), liver lysate (F), bile (G), feces (H) 21hrs after gavage of a mixture of cholesterol and ^{14}C-cholesterol. **I-K.** Transcriptomic profiling of livers from *Ldlr*$^{-/-}$ mice fed WD for 3 weeks, then orally gavaged with vehicle or amlexanox for 8 weeks with the continuation of WD feeding. **I.** Scatterplot for RNA-seq data. **J.** Functional annotation associated with genes expressed more highly in amlexanox-treated mice. **K.** Relative expression values (Z-scaled $\log_2$(TPM+1)) for genes involved in bile acid metabolism. **L.** Fecal bile acid levels in *Ldlr*$^{-/-}$ mice fed WD for 3 weeks, then orally gavaged with vehicle or amlexanox for 8 weeks with the continuation of WD feeding. Mean ± SEM. *, P<0.05, Student's unpaired t test.

Fig. 3

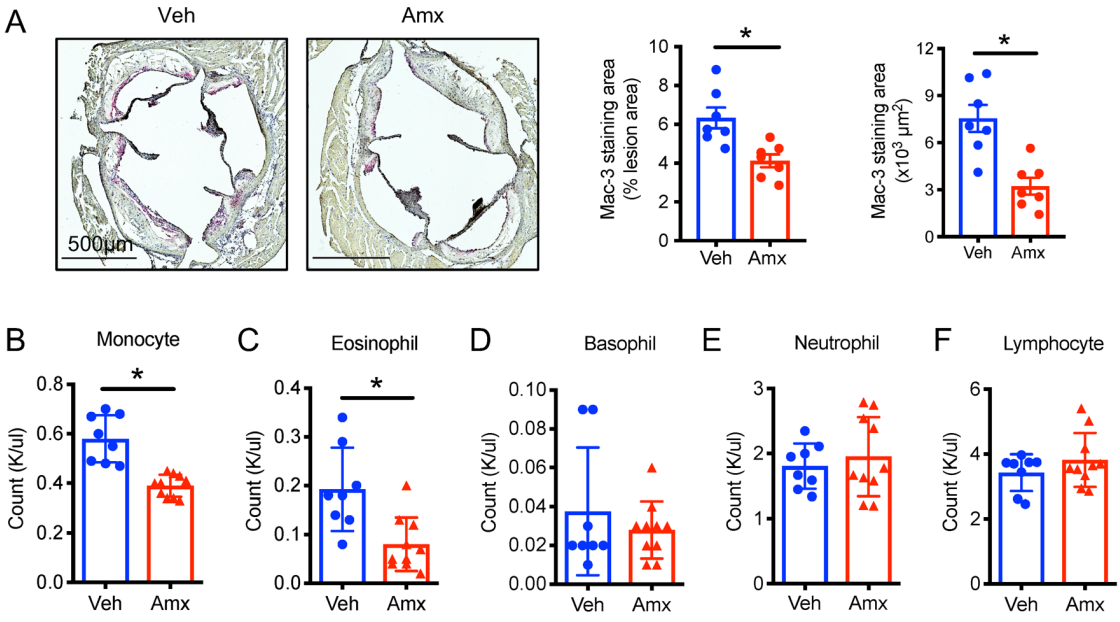
A
Veh
Amx
500μm
Mac-3 staining area (% lesion area)
Mac-3 staining area (x10³ μm²)
Veh
Amx
B
Monocyte
C
Eosinophil
D
Basophil
E
Neutrophil
F
Lymphocyte
Count (K/ul)

Figure 3. Amlexanox reduces circulating monocytes and lesion macrophage. *Ldlr*$^{-/-}$ mice were fed WD for 3 weeks, then orally gavaged with vehicle or amlexanox for 8 weeks with the continuation of WD feeding. **A.** Mac-3 staining of aortic roots and quantification. **B-F.** Complete blood count of circulating immune cells: monocytes (B), eosinophils (C), basophils (D), neutrophils (E), lymphocytes (F). Mean ± SEM. *, $P<0.05$, Student's unpaired *t* test.

Fig. 4

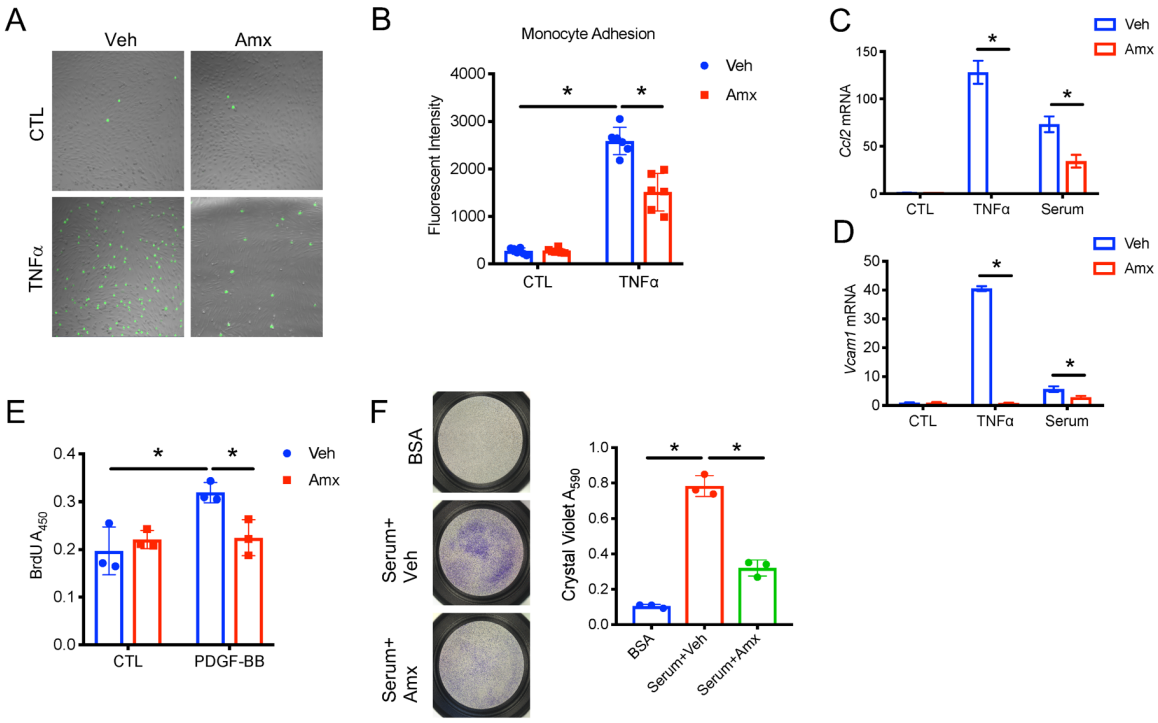
A
Veh
Amx
CTL
TNFα
B
Monocyte Adhesion
Fluorescent Intensity
4000
3000
2000
1000
0
Veh
Amx
CTL
TNFα
C
Ccl2 mRNA
150
100
50
0
CTL
TNFα
Serum
Veh
Amx
D
Vcam1 mRNA
50
40
30
20
10
0
CTL
TNFα
Serum
Veh
Amx
E
BrdU A450
0.4
0.3
0.2
0.1
0.0
CTL
PDGF-BB
Veh
Amx
F
BSA
Serum+ Veh
Serum+ Amx
Crystal Violet A590
1.0
0.8
0.6
0.4
0.2
0.0
BSA
Serum+Veh
Serum+Amx

Figure 4. Amlexanox prevents dysfunction of aortic vessel cells. A-B. THP-1 monocyte labeled with BCECF was co-cultured with Human aortic endothelial cells pretreated with vehicle or 100μM amlexanox, then treated with 10ng/ml TNFα for 16hrs. Monocyte adhesion was visualized by confocal microscopy (A), or examined by the measurement of fluorescent intensity (B). **C-D.** *Vcam1* (C) and *Ccl2* (D) expression in HAECs treated with 5nM TNFα or 10% serum in the presence of vehicle or 100μM amlexanox. **E.** BrdU proliferation assay on mouse aortic SMC pretreated with Vehicle or 100μM Amlexanox, then treated with 20ng/ml PDGF-BB for 24hrs. **F.** Transwell migration assay of SMC pretreated with vehicle or 100μM amlexanox, then treated with serum from WD-fed *Ldlr*$^{-/-}$ mice. Mean ± SD. *, $P<0.05$, Student's unpaired *t* test.

Fig. 5

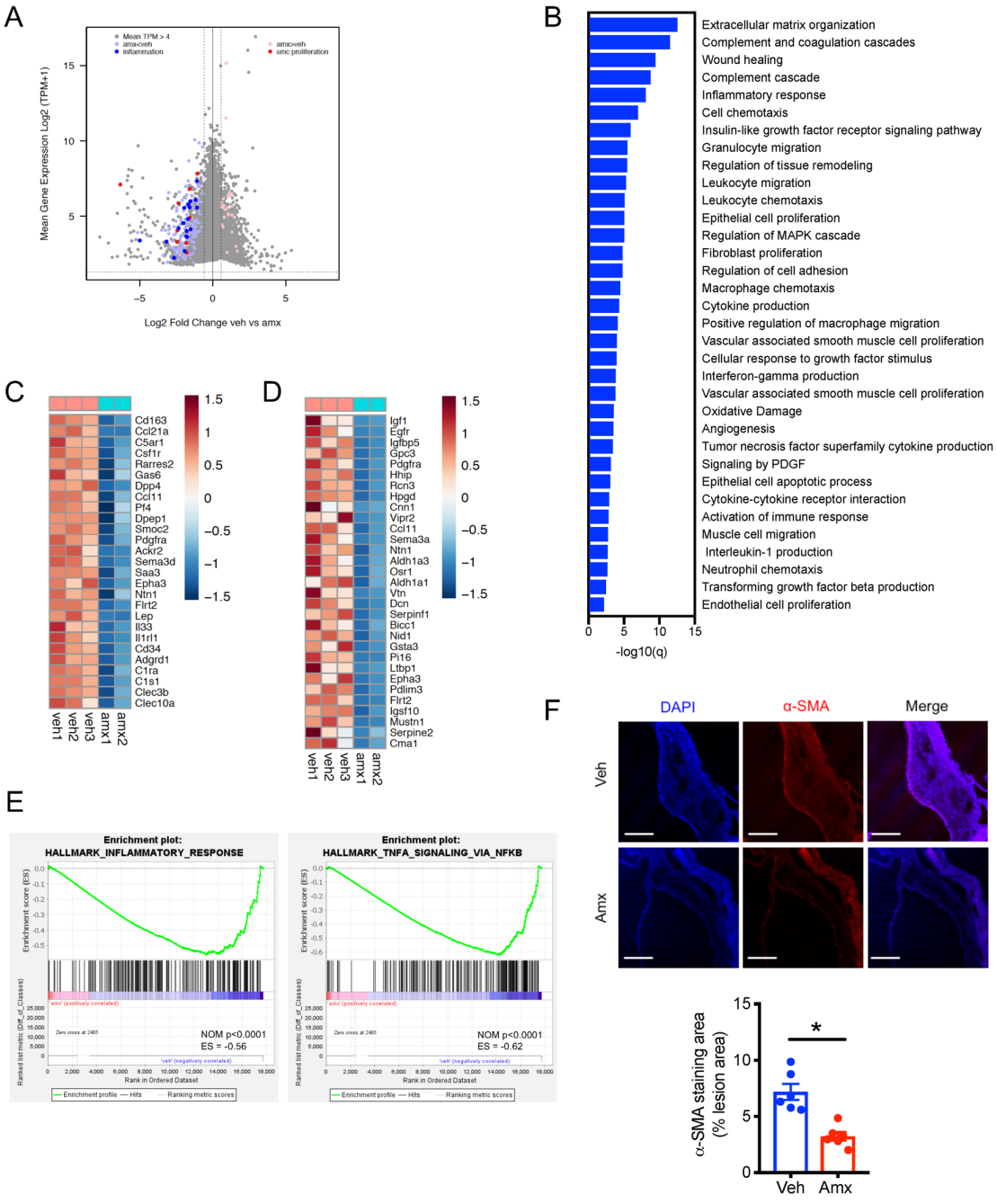
A
Mean TPM > 4
amx>veh
inflammation
amx>veh
smc proliferation
Mean Gene Expression Log2 (TPM+1)
Log2 Fold Change veh vs amx
B
Extracellular matrix organization
Complement and coagulation cascades
Wound healing
Complement cascade
Inflammatory response
Cell chemotaxis
Insulin-like growth factor receptor signaling pathway
Granulocyte migration
Regulation of tissue remodeling
Leukocyte migration
Leukocyte chemotaxis
Epithelial cell proliferation
Regulation of MAPK cascade
Fibroblast proliferation
Regulation of cell adhesion
Macrophage chemotaxis
Cytokine production
Positive regulation of macrophage migration
Vascular associated smooth muscle cell proliferation
Cellular response to growth factor stimulus
Interferon-gamma production
Vascular associated smooth muscle cell proliferation
Oxidative Damage
Angiogenesis
Tumor necrosis factor superfamily cytokine production
Signaling by PDGF
Epithelial cell apoptotic process
Cytokine-cytokine receptor interaction
Activation of immune response
Muscle cell migration
Interleukin-1 production
Neutrophil chemotaxis
Transforming growth factor beta production
Endothelial cell proliferation
-log10(q)
C
Cd163
Ccl21a
C5ar1
Csf1r
Rarres2
Gas6
Dpp4
Ccl11
Pf4
Dpep1
Smoc2
Pdgfra
Ackr2
Sema3d
Saa3
Epha3
Ntn1
Flrt2
Lep
Il33
Il1rl1
Cd34
Adgrd1
C1ra
C1s1
Clec3b
Clec10a
veh1
veh2
veh3
amx1
amx2
D
Igf1
Egfr
Igfbp5
Gpc3
Pdgfra
Hhip
Rcn3
Hpgd
Cnn1
Vipr2
Ccl11
Sema3a
Ntn1
Aldh1a3
Osr1
Aldh1a1
Vtn
Dcn
Serpinf1
Bicc1
Nid1
Gsta3
Pi16
Ltbp1
Epha3
Pdlim3
Flrt2
Igsf10
Mustn1
Serpine2
Cma1
E
Enrichment plot:
HALLMARK_INFLAMMATORY_RESPONSE
NOM p<0.0001
ES = -0.56
Enrichment plot:
HALLMARK_TNFA_SIGNALING_VIA_NFKB
NOM p<0.0001
ES = -0.62
Enrichment score (ES)
Ranked list metric (Diff_of_Classes)
Rank in Ordered Dataset
Enrichment profile
Hits
Ranking metric scores
F
DAPI
α-SMA
Merge
Veh
Amx
α-SMA staining area
(% lesion area)
Veh
Amx

Figure 5. Amlexanox affects aortic transcriptome during atherogenesis. A-E. Transcriptomic profiling of aorta from *Ldlr*$^{-/-}$ mice fed WD for 3 weeks, then orally gavaged with vehicle or amlexanox for 8 weeks with the continuation of WD feeding. **A.** MA plot of mRNA expression. **B.** Functional annotation associated with genes expressed lower in amlexanox-treated mice. **C, D.** Relative expression values (Z-scaled $\log_2$(TPM+1)) for genes involved in inflammation (C) or SMC proliferation and migration (D). **E.** Gene Set Enrichment Analysis of differentially expressed transcripts related to inflammatory response and TNFα signaling in aorta of vehicle or amlexanox-treated WD-fed *Ldlr*$^{-/-}$ mice. **F.** α-SMA staining of aortic roots and quantification. Scale bar, 200μm. *Ldlr*$^{-/-}$ mice were fed WD for 3 weeks, then orally gavaged with vehicle or amlexanox for 8 weeks with the continuation of WD feeding. Mean ± SEM. *, P<0.05, Student's unpaired *t* test.

Supplementary Fig. 1

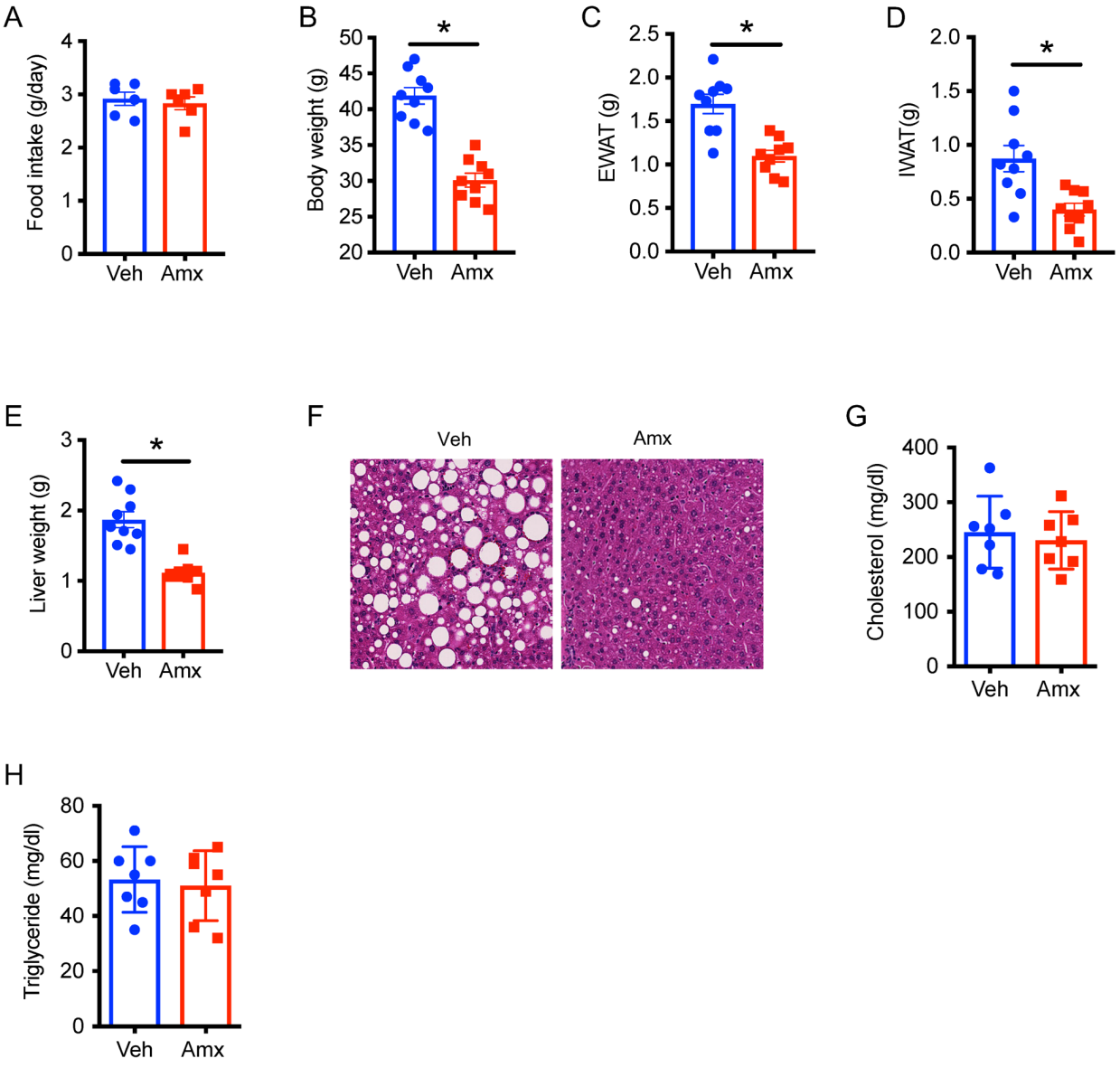

Supplementary Figure 1. Amlexanox reduces body weight and fat mass in mice fed with Western diet. A-F. *Ldlr*$^{-/-}$ mice were fed WD for 3 weeks, then orally gavaged with vehicle or amlexanox for 8 weeks with the continuation of WD feeding. **A.** Food intake. **B.** Body weight. **C.** Weight of epididymal white adipose tissue. **D.** Weight of inguinal white adipose tissues. **E.** Liver weight. **F.** H&E staining of liver sections. **G-H.** *Ldlr*$^{-/-}$ mice were fed normal chow diet for 3 weeks, then orally gavaged with vehicle or amlexanox for 8 weeks with the continuation of chow diet feeding. **G.** Fasting serum cholesterol. **H.** Fasting serum triglyceride. Mean ± SEM. *, $P<0.05$, Student's unpaired *t* test.

Supplementary Fig. 2

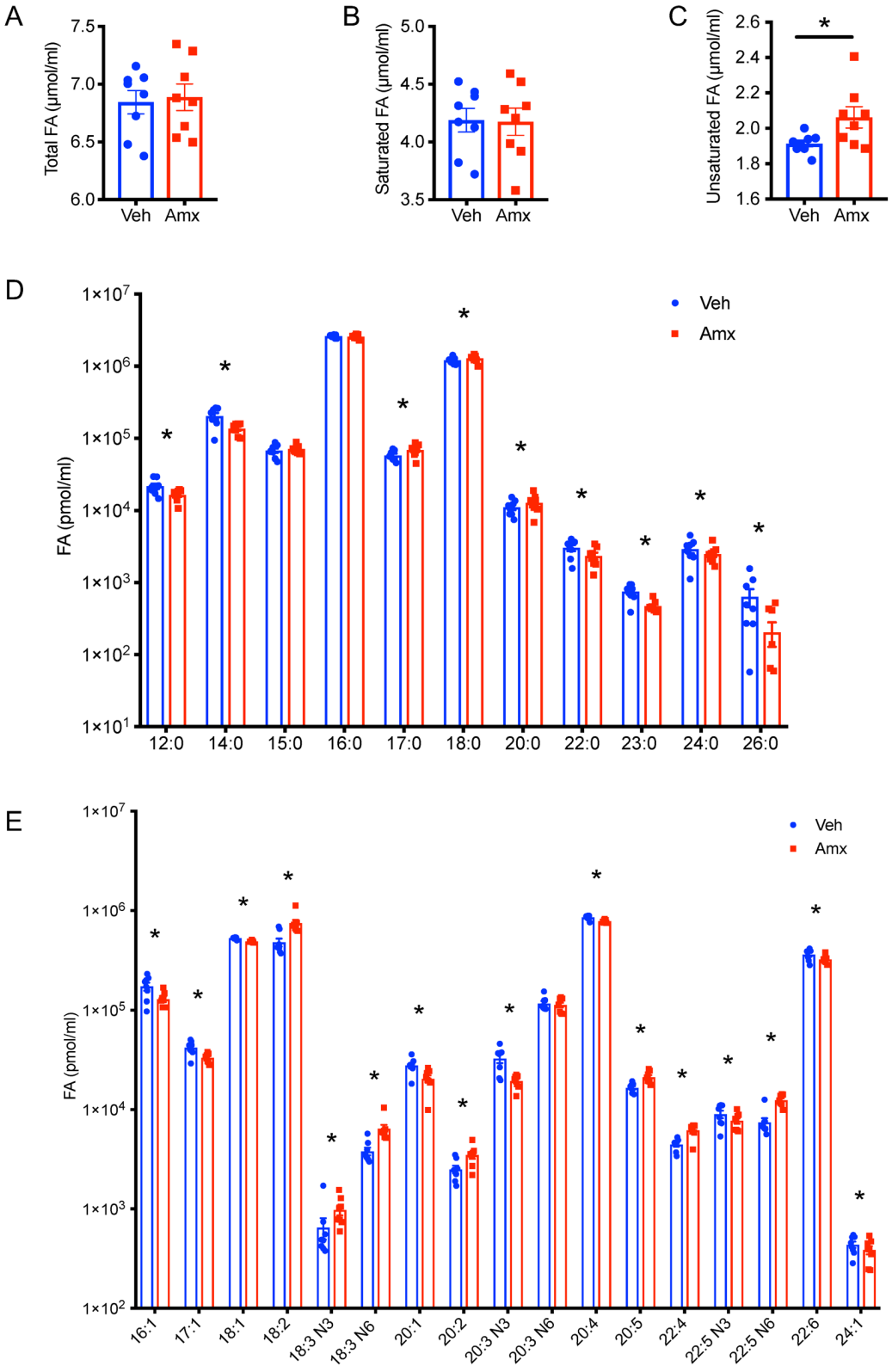

Supplementary Figure 2. The effects of amlexanox on circulating levels of total fatty acids. Lipidomic profiling of plasma from fasted *Ldlr*$^{-/-}$ mice fed WD for 3 weeks, then orally gavaged with vehicle or amlexanox for 8 weeks with the continuation of WD feeding. **A.** Total fatty acids. **B.** Saturated fatty acids. **C.** Unsaturated fatty acids. **D.** Species of saturated fatty acids. **E.** Species of unsaturated fatty acids. Mean ± SEM. *, $P<0.05$, Student's unpaired *t* test.

Supplementary Fig. 3

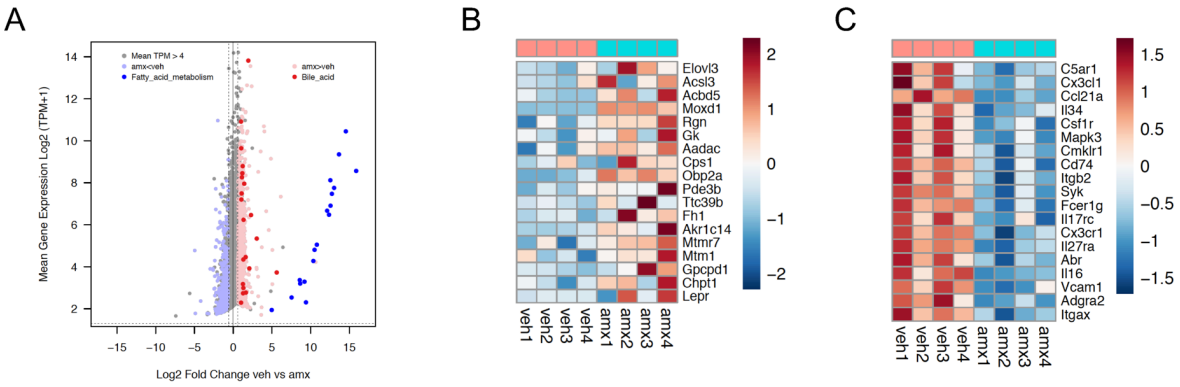

Supplementary Figure 3. Amlexanox affects hepatic transcriptome. Transcriptomic profiling of livers from *Ldlr*$^{-/-}$ mice fed WD for 3 weeks, then orally gavaged with vehicle or amlexanox for 8 weeks with the continuation of WD feeding. **A.** MA plot of RNA-seq data. **B, C.** Relative expression values (Z-scaled $\log_2$(TPM+1)) for genes involved in fatty acid metabolism (B) or inflammation (C).

Supplementary Fig. 4

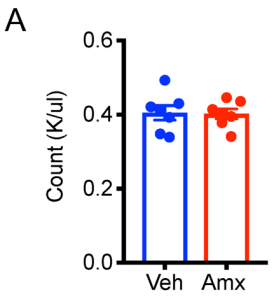

Supplementary Figure 4. Amlexanox does not affect the number of circulating monocytes in mice fed chow diet. Circulating monocytes in *Ldlr*$^{-/-}$ mice were fed normal chow diet for 3 weeks, then orally gavaged with vehicle or amlexanox for 8 weeks with the continuation of feeding.

Supplementary Fig. 5

A

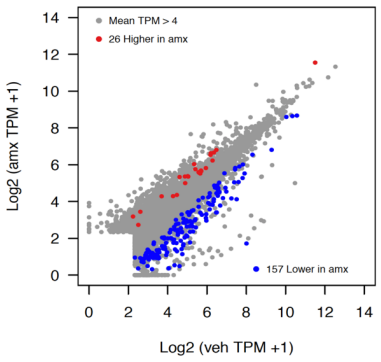

B

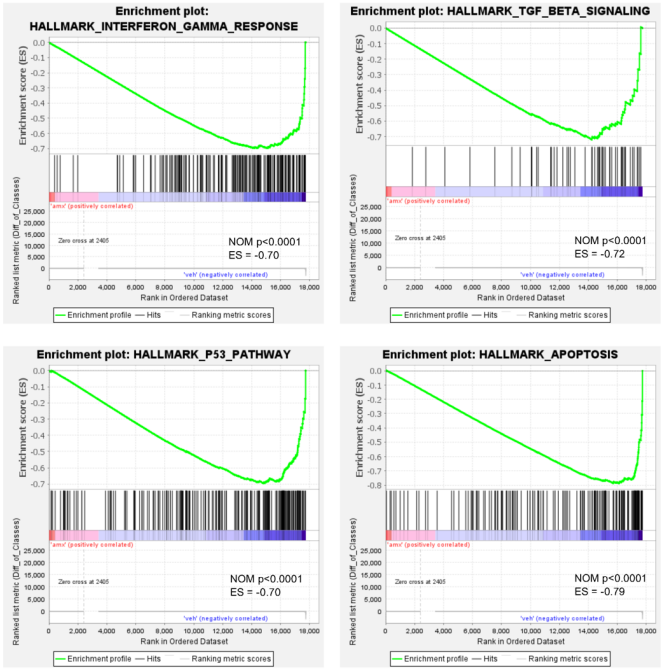

Supplementary Figure 5. Amlexanox affects transcriptome of aortic vessel. Transcriptomic profiling of aorta from *Ldlr*$^{-/-}$ mice fed WD for 3 weeks, then orally gavaged with vehicle or amlexanox for 8 weeks with the continuation of WD feeding. **A.** Scatterplot of RNA-seq data. **B.** Gene Set Enrichment Analysis of differentially expressed transcripts related to interferon gamma response, TGFβ signaling, P53 pathway and apoptosis in aorta of vehicle or amlexanox treated WD-fed *Ldlr*$^{-/-}$ mice.